ScAlN Thick-Film Ultrasonic Transducer in 40–80 MHz

Ko-hei Sano, Rei Karasawa, and Takahiko Yanagitani

***Abstract*— A medical ultrasound diagnostic system and an ultrasonic microscope are generally used in the frequency range of 1–20 MHz and 100 MHz–2 GHz, respectively. Ultrasonic transducers in the frequency range of 20–100 MHz are, therefore, not well developed because of less application into ultrasonic imaging or suitable piezoelectric materials with this frequency range. Polyvinylidene difluoride (PVDF) is usually used for ultrasonic transducers in the 10–50-MHz ranges. However, their electromechanical coupling coefficient k_t^2 of 4% is not enough for the practical uses. In order to excite the ultrasonic wave in the 20–100 MHz range, a 125–25-μm-thick piezoelectric film is required when the longitudinal velocity of the material is assumed to be 5000 m/s. However, it is difficult to grow such a thick piezoelectric film without a crack being caused by the internal stress during the dry deposition technique. We achieved a stress-free film growth by employing the unique hot target sputtering technique without heating the substrate. High-efficient 81- (k_t^2 = 18.5%) and 43-MHz (k_t^2 = 15.2%) ultrasonic generation by using the 43- and 90-μm extremely thick ScAlN (Sc: 39%) films were demonstrated, respectively. We discussed the advantage of ScAlN thick-film transducers by comparing them with the conventional PVDF transducer for the water medium.**

***Index Terms*— Piezoelectric films, piezoelectric resonators, ScAlN, sputtering, thick piezoelectric film, ultrasonic transducer.**

I. Introduction

A RESOLUTION of ultrasonic image and measurement depth depends on a frequency range of a transducer. A medical ultrasound diagnostic system usually observes internal organs placed more than 3 mm deep using the frequency range of 1–20-MHz ultrasonic waves. An ultrasonic microscope can observe 10-μm-thick tissue using the frequency range of 100 MHz–2 GHz. The demand for the frequency range of 20–100 MHz is nowadays increasing for high-resolution imaging applications which can visualize tissues *in vivo* such as skin layers [1], [2], blood vessels [3], and corneal tissues [4]. An ultrasonic transducer shows the highest conversion efficiency in the acoustic resonant frequency. The thickness extensional resonant frequency is determined by its material thickness (d) and longitudinal wave velocity (v). The half-wavelength resonant frequency f_0 is given by $v/2d$. Therefore, 25-μm thickness is required for the ultrasonic transducer operating at the resonance frequency of 100 MHz when the longitudinal velocity is assumed to be 5000 m/s. In order to fabricate such a thick film, there are two approaches. One is to thin down single crystal plates and the other is to grow thick piezoelectric films. Lim and Shung [5] reported the 7.1-μm-thick polished $LiNbO_3$ single crystal focused transducer operating at 410 MHz for the evaluation of interactive forces of red blood cells. Chen *et al.* [6] reported the mechanically polished $LiNbO_3$ single crystal focused transducer operating at 526 MHz for microparticle manipulation applications. Although they reported the focused transducers in the mechanical polishing approach, it may not be easy to adhere piezoelectric plates to a complicated surface such as curved and concaved surfaces, e.g., acoustic lens. A thick-film approach allows us to obtain a thick piezoelectric layer on a complicated surface. However, the fabrication of such a thick film is difficult because the cracks are usually formed in the film caused by the internal stress during the dry deposition technique. In previous study, high piezoelectricity ($k_t^2 = 30\%$ at 82 MHz [7] and $k_t^2 = 26\%$ at 50–70 MHz [8], [9]) was reported in the PMN-PT or PZT thick film by using wet coating processes and hydrothermal synthesis methods, respectively. High k_t^2 of 19% was also reported in the Li-doped KNN thick films operating at 52 MHz. Extremely high k_t^2 of 35% was reported in the sol-gel-deposited thin PZT films for FBAR applications [10], [11]. Although polyvinylidene difluoride (PVDF) polymer membranes are suitable for use in ultrasonic transducers in the 10–50 MHz, their electromechanical coupling coefficient k_t^2 of 4% is not large [12].

A large piezoelectricity of ScAlN thin film has been reported in [13]. The piezoelectric property is improved by increasing the Sc concentration. Its piezoelectricity reaches a maximum when the Sc/Al concentration is approximately 43% which is near the phase boundary between wurtzite and cubical crystal. We have first reported the fabrication of the ultrasonic transducer and FBAR using the ScAlN thin film, and demonstrated high piezoelectricity (k_t^2 = 15% [14]), in 2010. A high-frequency ultrasonic transducer such as a micromachined ultrasonic transducer using the AlN thin film and focused transducer using ScAlN thin film are recently reported [15], [16].

In this paper, two types of 39% Sc-doped ScAlN thick piezoelectric film ultrasonic transducer using a thin substrate and rod-shaped substrate were fabricated by using the hot target sputtering technique. The electromechanical coupling

Manuscript received January 26, 2018; accepted July 9, 2018. Date of publication August 24, 2018; date of current version November 7, 2018. This work was supported in part by the Japan Science and Technology Agency, PRESTO under Grant JPMJPR16R8 and in part by JSPS KAKENHI under Grant 16H04356 and Grant 18K19037. *(Corresponding author: Takahiko Yanagitani.)*

K.-h. Sano and R. Karasawa are with the Graduate School of Advanced Science and Engineering, Waseda University, Tokyo 169-8555, Japan.

T. Yanagitani is with the Graduate School of Advanced Science and Engineering, Waseda University, Tokyo 169-8555, Japan, also with JST-PRESTO, Saitama 332-0012, Japan, and also with ZAIKEN, Tokyo 169-0051, Japan (e-mail: yanagitani@waseda.jp).

Digital Object Identifier 10.1109/TUFFC.2018.2865791

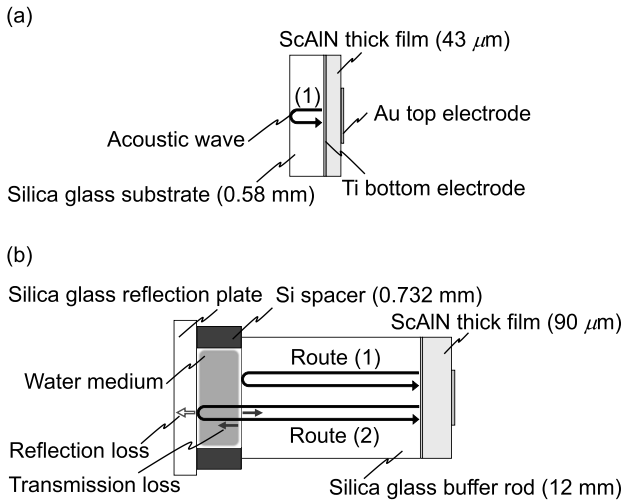

Fig. 1. We fabricated two samples: (a) thin substrate sample and (b) transducer sample. Structure of ScAlN thick-film transducer consisting of Au top electrode/ScAlN thick film/Ti bottom electrode/(a) thin silica glass substrate (0.58 mm) or (b) silica glass buffer rod (9 mm diameter × 12 mm).

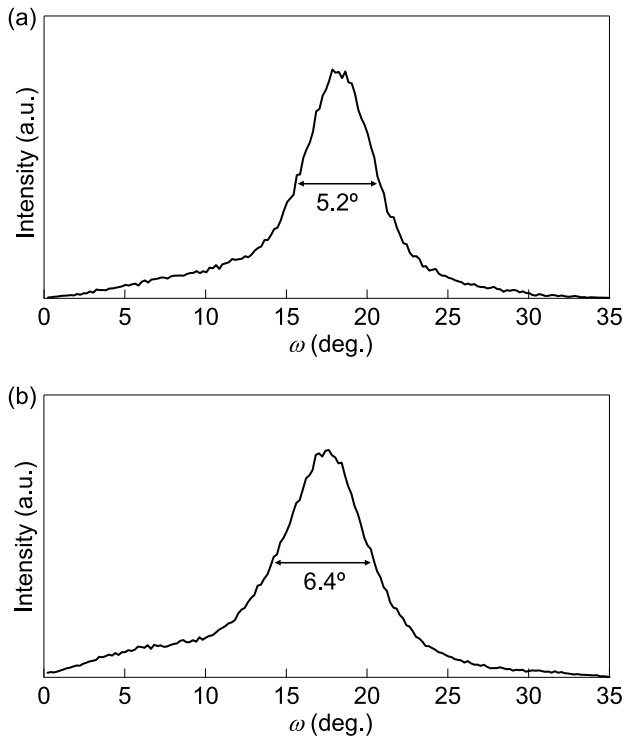

Fig. 2. (0002) plane ω-scan rocking curve of (a) 43-μm ScAlN thick film (thin substrate sample) measured at $\chi = 1.3°$ and (b) 90-μm ScAlN thick film (transducer sample) measured at $\chi = 3.0°$. χ angle indicates c-axis tilt angle to the surface normal.

coefficient k_t^2 of ScAlN thick films was determined by comparing from experimental conversion loss with a theoretical one [17]. We demonstrated high-efficient 81- and 43-MHz ultrasonic generation by using 43 and 90 μm extremely thick ScAlN films, respectively. In addition, we fabricated the 40-MHz ultrasonic transducer consisting of the ScAlN thick film (90 μm) and silica glass buffer rod to characterize the transducer performance in water mediums.

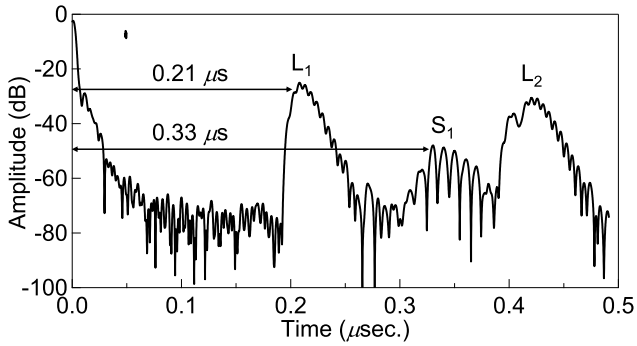

Fig. 3. Time-domain impulse response obtained from an inverse Fourier transform of S_{11} measured by a network analyzer. L_1: first echo of the longitudinal wave. S_1: shear wave reflected from the bottom of silica glass substrate.

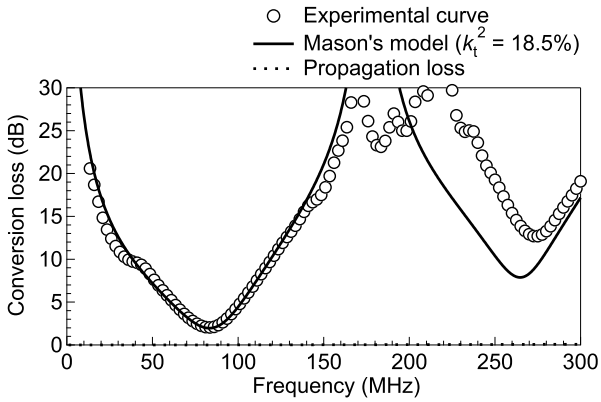

Fig. 4. Experimental and theoretical conversion loss curves of the transducer consisting of Au top electrode/43-μm ScAlN thick film/Ti bottom electrode/0.58-mm silica glass substrate (thin substrate sample).

II. ScAlN Thick-Film Growth

Before the transducer (rod shape substrate) fabrication, to examine k_t^2 of the ScAlN films, by using the thin substrate (0.58 mm thick), a 43-μm-thick film was grown on highly oriented (0001) Ti electrode films [XRD rocking curve full-width at half-maximum (FWHM) = 3.5°]/silica glass substrate ($25 \times 50 \times 0.58$ mm^3) (thin substrate sample), as shown in Fig. 1(a). In the transducer fabrication, a 90-μm-thick ScAlN film was grown on (0001) Ti electrode film/silica glass buffer rod(9 mm diameter × 12 mm) (transducer sample), as shown in Fig. 1(b). We employed the hot target RF magnetron sputtering technique for the film growth. The advantage of the hot target sputtering process is high-density plasma caused by the thermal electron emission from a sputtering target. The hot target condition was obtained by introducing a gap between the target and the water-cooled magnetron cathode. In this case, the target was cooled sufficiently, a crack was observed when the thickness of the films reaches 8 μm. Typical target temperature measured by an infrared thermometer during the sputtering were approximately 400 °C, 510 °C, and 470 °C, at center, erosion area, and rim of the target, respectively. A single sputtering source with a 3-in ScAl alloy metal target (Sc/Al = 43%) was used. Since pure metal Sc is easily oxidized, energetic negative oxygen ions are generated. We reported that these negative ion bombardments

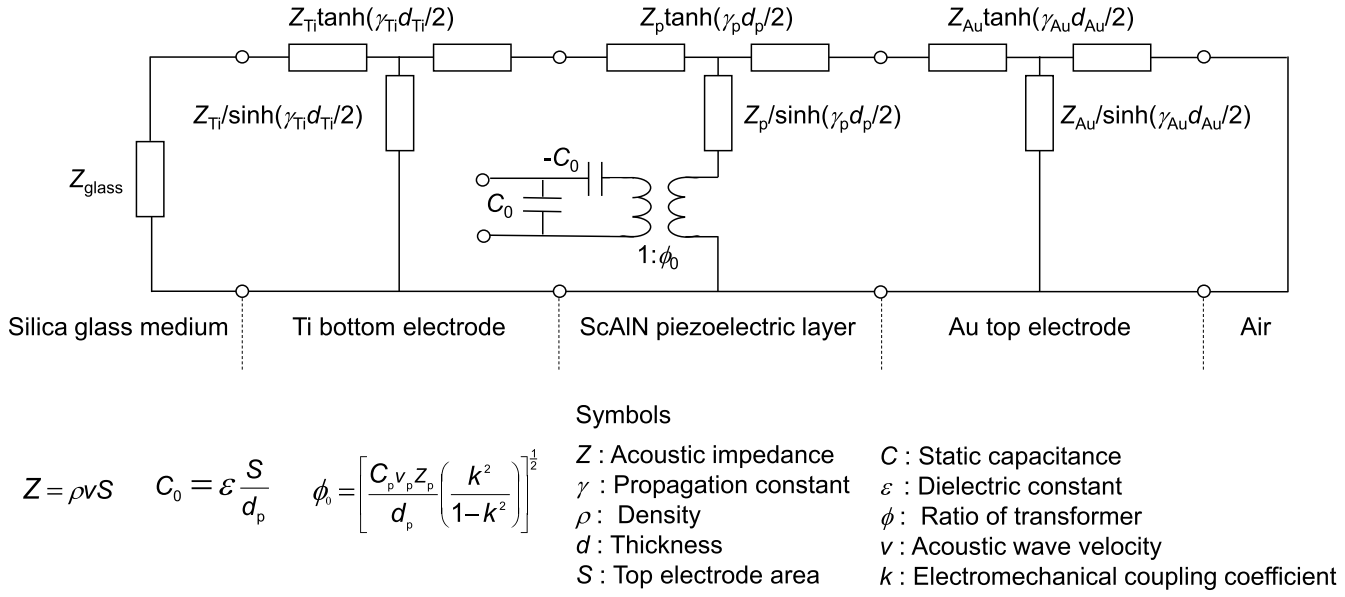

Fig. 5. Mason's equivalent circuit model of the transducer consisting of silica glass substrate (infinite)/Ti bottom electrode/ScAlN piezoelectric layer/air (infinite). This model indicates the transducer as shown in Fig. 1(a) and route (1) in Fig. 1(b).

TABLE I
SPUTTERING CONDITION OF ScAlN THICK-FILM GROWTH

Growth condition	ScAlN (43 μm)	ScAlN (90 μm)
Sample name	Thin substrate	Transducer
Substrate	Silica glass plate	Silica glass rod
Substrate size (mm)	25×50×0.58	9 mm dia.×12
RF power	150−250 W	100−250 W
Ratio of pressure (Ar/N_2)	2	2
Gas pressure	0.5 Pa	0.5 Pa
Substrate heating	None	None
Substrate-target distance	25 mm	25 mm
Deposition time	23.5 hours	50 hours

TABLE II
COMPARISON OF ELECTROMECHANICAL COUPLING COEFFICIENT OF PIEZOELECTRIC FILM MATERIALS

	k_t^2	Reference
PMN-PT (PT:33%)	30%	[7]
PZT (hydrothermal synthesis)	26%	[8]
PZT (sol-gel)	35%	[11]
PVDF polymer membrane	4%	[12]
ZnO (single crystal)	8.4%	[22]
AlN (single crystal)	6.0%	[23]
ScAlN thin film	15%	[14]
ScAlN thick film (43 μm)	18.5%	This work

to the substrate degrade the crystalline orientation of ScAlN films [18]. We previously found that the negative ion bombardment was suppressed when the ScAl alloy target was used [18]. Table I shows the film growth condition. The thickness of the films was controlled by deposition time and RF power. These thicknesses of films (both thin substrate sample and transducer sample) were measured by using a stylus profiler (Dektak XT-S). The Sc concentration of these thick films was measured to be 39% using fluorescent X-ray analysis (ZSX-Primus II, Rigaku). This concentration is near the reported morphotropic phase boundary where the highest electromechanical coupling appears [19]. Fig. 2(a) and (b) shows the (0002) plane ω-scan rocking curve measured for the thin substrate sample and transducer sample. The FWHM of the curves was measured to be 5.2° and 6.4°, respectively.

III. ELECTROMECHANICAL COUPLING COEFFICIENT k_t^2 OF ScAlN THICK FILM (THIN SUBSTRATE SAMPLE)

In order to examine k_t^2 of the thick ScAlN films, the ultrasonic transducer consisting of thin silica glass substrate (0.58 mm) was prepared, as shown in Fig. 1(a). k_t^2 of the thick film was determined by comparing the experimental with theoretical longitudinal wave conversion losses. The experimental conversion losses were measured using a network analyzer (E5071C, Agilent Technologies). At first, the time-domain impulse response was obtained by an inverse Fourier transform of S_{11}, as shown in Fig. 3. Echo signals multireflected between the surface and the bottom of the substrate were observed periodically with 0.21 μs. These responses determined to be a longitudinal wave by using the longitudinal velocity (ScAlN: 7530 m/s [19] and silica glass: 5957 m/s [20]) and the thicknesses of the transducer (ScAlN

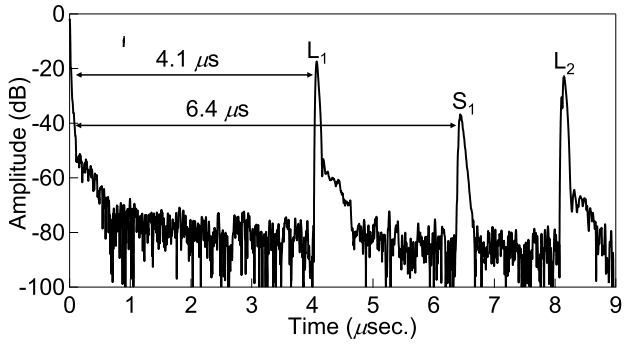

Fig. 6. Time-domain impulse response obtained from an inverse Fourier transform of S_{11}. L_1: first echo of the longitudinal wave. L_2: second echo of the longitudinal wave. S_1: shear wave reflected from the bottom of silica glass substrate.

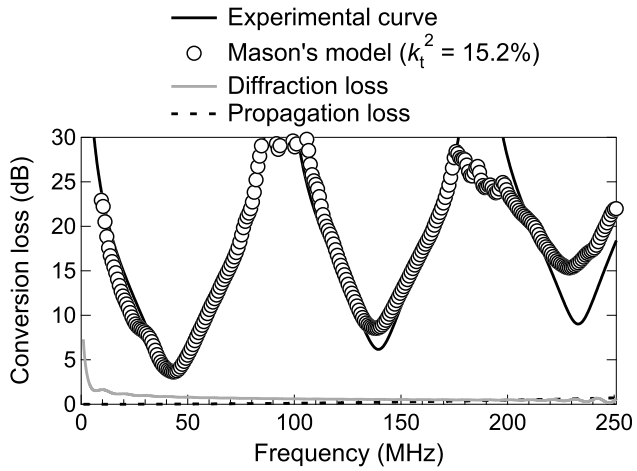

Fig. 7. Experimental and theoretical conversion loss curves of the transducer sample consisting of Au top electrode/90-μm ScAlN thick film/Ti bottom electrode/12-mm silica glass buffer rod (transducer sample).

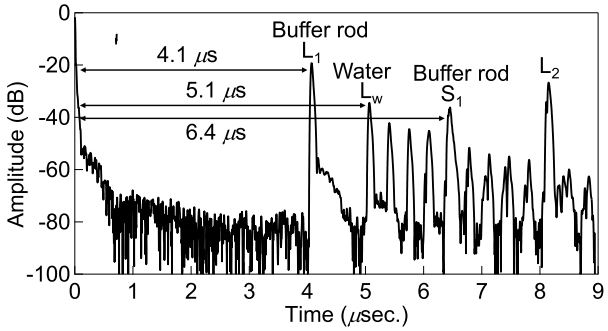

Fig. 8. Impulse response of ScAlN transducer after injecting the water medium. L_1: first echo of the longitudinal wave. L_2: second echo of the longitudinal wave. S_1: shear wave reflected from the bottom of silica glass substrate. L_w: first echo of the longitudinal wave reflected from the silica glass reflection plate.

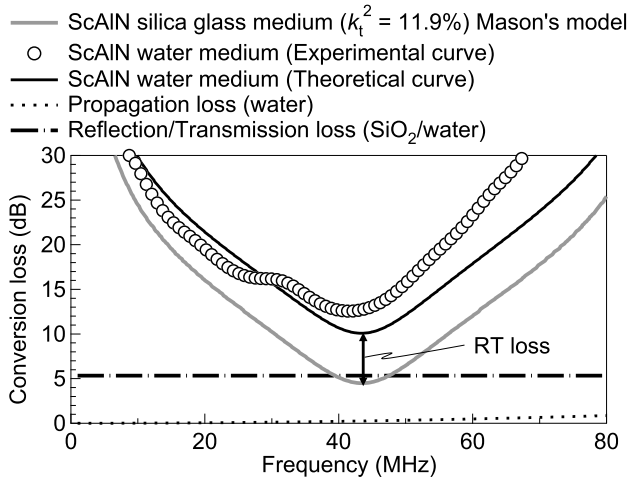

Fig. 9. Experimental and theoretical conversion loss curves of the ScAlN hydrophone. The theoretical conversion loss was obtained by subtracting the *RT loss* from the theoretical conversion loss without the water medium.

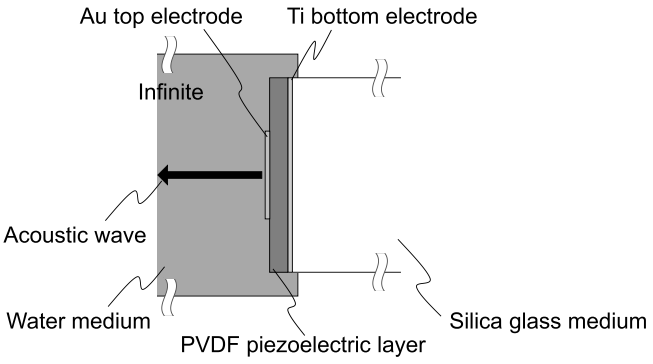

Fig. 10. Simulation model of PVDF transducer consisting of water medium (infinite)/Au top electrode/PVDF piezoelectric layer/silica glass medium (infinite).

film: 43 μm and silica glass substrate: 0.58 mm). The first echo was Fourier-transformed into the frequency domain to obtain the conversion loss curve, as shown in Fig. 4. The theoretical conversion loss curves of the transducer as shown in Fig. 1(a) were simulated using multilayered Mason's equivalent circuit model, as shown in Fig. 5. k_t^2 is determined by adjusting k_t in the model to match the theoretical conversion loss to the experimental one at a minimum point of the curves. The minimum points on the conversion loss curve show the thickness-extensional mode resonance frequencies. k_t^2 of the ScAlN thick film is determined as 18.5% at the resonance frequency of 81 MHz. Table II shows the comparison of electromechanical coupling coefficient of piezoelectric film material.

IV. ScAlN Thick-Film Transducer (Transducer Sample)

Ultrasonic transducers for biomedical imaging are generally used in contact with the water medium. Fig. 6 shows the time-domain impulse response of the ultrasonic transducer consisting of 90-μm ScAlN thick film and silica glass buffer rod (12 mm) (transducer sample) without water contacting. Longitudinal wave and shear wave echoes that reflect at the bottom of the silica glass buffer rod were periodically observed at 4.1 and 6.4 μs, respectively. Fig. 7 shows the experimental conversion loss of the transducer sample of route (1) in Fig. 1(b), which is obtained by the Fourier transform of the first longitudinal wave echo in Fig. 6. We can see the minimum value of the conversion loss curve at 43 MHz, indicating the thickness-extensional mode resonant frequency of the transducer. In the experimental conversion loss, propagation

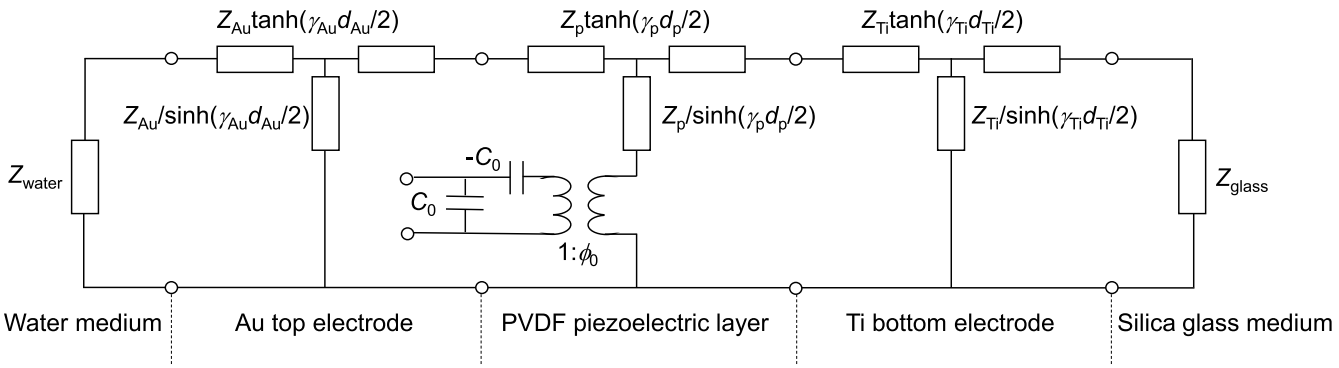

Fig. 11. Mason's equivalent circuit model of water medium (infinite)/Au top electrode/PVDF piezoelectric layer/silica glass medium (infinite).

loss and diffraction loss were subtracted. The propagation loss of the 12-mm silica glass rod was estimated by using $\alpha/f^2 = 1.6 \times 10^{-15}$ dB/s$^2 \cdot$ m [21]. Diffraction loss in the rod was estimated using Ogi's method as shown in Fig. 7. Experimental and theoretical conversion losses simulated by using the model shown in Fig. 5 showed a good agreement when k_t^2 is 15.2%.

A. Transducer Performance in Water Medium

Fig. 8 shows the impulse response after injecting the water medium. The reflected wave that propagates through the water medium and reflected at the surface of the silica glass reflection plate was clearly observed at 5.1 μs. The longitudinal conversion loss curve that was obtained by the Fourier transform of this wave was shown in Fig. 9. As shown in route (2) of Fig. 1(b), the acoustic wave reflected from the surface of the reflection plate propagates in the 12-mm silica glass buffer rod and the 0.72-mm water medium. Route (2) includes two transmission losses and one reflection loss, in addition to route (1). The theoretical conversion loss for route (2) was estimated by subtracting the reflection and transmission loss (*RT loss*) at the boundary between the silica glass buffer rod medium and the water medium from the theoretical conversion loss without the water medium [route (1)]. A ratio of transmission and reflection between two mediums is given by the following equations:

$$T = \frac{4Z_{\text{glass}}Z_{\text{water}}}{(Z_{\text{glass}} + Z_{\text{water}})^2} \quad (1)$$

$$R = 1 - T \quad (2)$$

where $Z_{\text{water}}(=\rho_{\text{water}}v_{\text{water}})$ and $Z_{\text{glass}}(=\rho_{\text{glass}}v_{\text{glass}})$ are acoustic impedances for the silica glass and water, respectively. The longitudinal wave velocity of the ScAlN, silica glass, and water used in the model was 8350, 5957, and 1500 m/s, respectively. The density of the ScAlN, silica glass, and water was set to be 3260, 2202, and 1000 kg/m^3, respectively. The RT loss was obtained by the following equations:

$$\text{RT loss} = -\frac{1}{2}(2 \times 10\log_{10} T + 10\log_{10} R) \quad (3)$$

$$10\log_{10} R = -2.00 \text{ dB} \quad (4)$$

$$10\log_{10} T = -4.34 \text{ dB} \quad (5)$$

$$\text{RT loss} = 5.33 \text{ dB}. \quad (6)$$

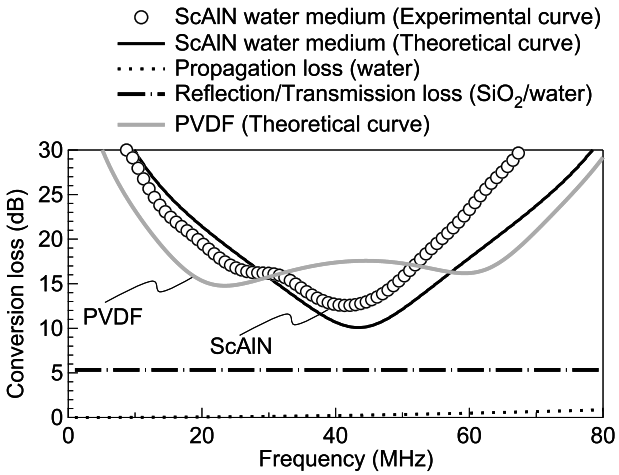

Fig. 12. Experimental and theoretical conversion loss of the ScAlN transducer and theoretical conversion loss curves of the ideal PVDF transducer simulated by using the model as shown in Fig. 11.

The experimental conversion loss is higher (worse) than that of theoretical prediction because the sound axis between the silica glass buffer rod and reflection plate was deviated. The buffer rod might not completely parallel to the reflection plate.

B. Comparison of the ScAlN Transducer With PVDF Transducer

In the frequency range of 20–100 MHz, PVDF transducers were used for ultrasonic imaging applications because of their easy fabrication of thick film and the low acoustic impedance close to the water medium. We compared the experimental conversion loss of ScAlN transducer with the simulated conversion loss of ideal PVDF transducer consisting of Au top electrode/PVDF piezoelectric layer/Ti bottom electrode/silica glass medium, as shown in Fig. 10. Mason's equivalent circuit model of the PVDF transducer used for the water medium was shown in Fig. 11. The advantage of PVDF transducers is better acoustic impedance matching to the water medium due to their low acoustic impedance. The longitudinal conversion loss of ScAlN transducer and ideal PVDF transducer was shown in Fig. 12. The minimum conversion loss of ideal PVDF transducer is 14.8 dB. On the other hand, the minimum conversion loss of ScAlN transducer is 12.6 dB. The ScAlN

thick-film transducer has significantly better efficiency than that of the ideal PVDF transducer which has better acoustic impedance matching to water, although large *RT loss* due to the large acoustic impedance mismatch was included in the ScAlN transducer.

V. Conclusion

We achieved a low-frequency ultrasonic generation in the range of 40–80 MHz from extremely thick ScAlN film fabricated using the hot target RF magnetron sputtering technique. The thickness of 43-μm ScAlN has k_t^2 of 18.5% in 81 MHz. k_t^2 of 18.5% is comparable to the PZT thin film ($k_t^2 = 16\%$). The conversion loss of the ScAlN thick-film (90 μm) transducer in the water medium is much better than that of the ideal PVDF transducer which is usually used for an ultrasonic imaging device. The limit of optical penetration length in the photoacoustic imaging is in the order of several mile meter lengths. The limit of observation length using 20–100-MHz ultrasonic imaging is also several mile meter lengths. Therefore, 40–80-MHz ScAlN thick-film transducers in this study are promising for photoacoustic imaging applications.

References

[1] D. H. Turnbull, B. G. Starkoski, K. A. Harasiewicz, G. R. Lockwood, and F. S. Foster, "Ultrasound backscatter microscope for skin imaging," in *Proc. IEEE Ultrason. Symp.*, vol. 2, Oct. 1993, pp. 985–988.

[2] M. Dyson, S. Moodley, L. Verjee, W. Verling, J. Weinman, and P. Wilson, "Wound healing assessment using 20 MHz ultrasound and photography," *Skin Res. Technol.*, vol. 9, pp. 116–121, May 2003.

[3] R. Gessner, M. Lukacs, M. Lee, E. Cherin, F. S. Foster, and P. A. Dayton, "High-resolution, high-contrast ultrasound imaging using a prototype dual-frequency transducer: *In vitro* and *in vivo* studies," *IEEE Trans. Ultrason., Ferroelectr., Freq. Control*, vol. 57, no. 8, pp. 1772–1781, Aug. 2010.

[4] E. Pavlatos, H. Chen, K. Clayson, X. Pan, and J. Liu, "Imaging corneal biomechanical responses to ocular pulse using high-frequency ultrasound," *IEEE Trans. Med. Imag.*, vol. 37, no. 2, pp. 663–670, Feb. 2018.

[5] H. G. Lim and K. K. Shung, "Quantification of inter-erythrocyte forces with ultra-high frequency (410 MHz) single beam acoustic tweezer," *Ann. Biomed. Eng.*, vol. 45, no. 9, pp. 2174–2183, Sep. 2017.

[6] X. Chen *et al.*, "An adjustable multi-scale single beam acoustic tweezers based on ultrahigh frequency ultrasonic transducer," *Biotechnol. Bioeng.*, vol. 114, no. 11, pp. 2637–2647, Nov. 2017.

[7] X. Li *et al.*, "80-MHz intravascular ultrasound transducer using PMN-PT free-standing film," *IEEE Trans. Ultrason., Ferroelectr., Freq. Control*, vol. 58, no. 11, pp. 2281–2288, Nov. 2011.

[8] B. Zhu *et al.*, "Micro-particle manipulation by single beam acoustic tweezers based on hydrothermal PZT thick film," *AIP Adv.*, vol. 6, no. 3, p. 035102, 2016.

[9] B. P. Zhu, Q. F. Zhou, J. Shi, K. K. Shung, S. Irisawa, and S. Takeuchi, "Self-separated hydrothermal lead zirconate titanate thick films for high frequency transducer applications," *Appl. Phys. Lett.*, vol. 94, no. 10, p. 102901, 2009.

[10] B. Zhu *et al.*, "(100)-Textured KNN-based thick film with enhanced piezoelectric property for intravascular ultrasound imaging," *Appl. Phys. Lett.*, vol. 106, no. 17, p. 173504, 2015.

[11] J. D. Larson, III, S. R. Gilbert, and B. Xu, "PZT material properties at UHF and microwave frequencies derived from FBAR measurements," in *Proc. IEEE Ultrason. Symp.*, Aug. 2004, pp. 173–177.

[12] H. Ohigashi, "Electromechanical properties of polarized polyvinylidene fluoride films as studied by the piezoelectric resonance method," *J. Appl. Phys.*, vol. 47, no. 3, pp. 949–955, 1976.

[13] M. Akiyama, T. Kamohara, K. Kano, A. Teshigahara, Y. Takeushi, and N. Kawahara, "Enhancement of piezoelectric response in scandium aluminum nitride alloy thin films prepared by dual reactive cosputtering," *Adv. Mater.*, vol. 21, no. 5, pp. 593–596, Feb. 2008.

[14] T. Yanagitani, K. Arakawa, K. Kano, A. Teshigahara, and M. Akiyama, "Giant shear mode electromechanical coupling coefficient k_{15} in c-axis tilted ScAlN films," in *Proc. IEEE Ultrason. Symp.*, Oct. 2010, pp. 2095–2098.

[15] L. Lou, H. Yu, M. T. X. Haw, S. Zhang, and Y. A. Gu, "Comparative characterization of bimorph and unimorph AlN piezoelectric micromachined ultrasonic transducers," in *Proc. IEEE Micro Electro Mech. Syst.*, Jan. 2016, pp. 1090–1093.

[16] B. Zhu *et al.*, "Self-focused AlScN film ultrasound transducer for individual cell manipulation," *ACS Sens.*, vol. 2, no. 1, pp. 172–177, May 2017.

[17] T. Yanagitani, M. Kiuchi, M. Matsukawa, and Y. Watanabe, "Shear mode electromechanical coupling coefficient k_{15} and crystallites alignment of $(11\bar{2}0)$ textured ZnO films," *J. Appl. Phys.*, vol. 102, no. 2, pp. 024110-1–024110-7, Jul. 2007.

[18] S. Takayanagi, M. Matsukawa, and T. Yanagitani, "Effects of energetic negative ions generated from sputtering targets on ScAlN film growth," in *Proc. IEEE Ultrason. Symp.*, Sep. 2016, pp. 1–4.

[19] T. Yanagitani and M. Suzuki, "Electromechanical coupling and gigahertz elastic properties of ScAlN films near phase boundary," *Appl. Phys. Lett.*, vol. 105, no. 12, pp. 122907-1–122907-4, Sep. 2014.

[20] J. Kushibiki, T. Wei, Y. Ohashi, and A. Tada, "Ultrasonic microspectroscopy characterization of silica glass," *J. Appl. Phys.*, vol. 87, no. 6, pp. 3113–3121, Mar. 2000.

[21] B. A. Auld, *Acoustic Fields and Waves in Solids*, vol. 1. Hoboken, NJ, USA: Wiley, 1973, p. 92.

[22] R. T. Smith and V. E. Stubblefield, "Temperature dependence of the electroacoustical constants of Li-doped ZnO single crystals," *J. Acoust. Soc. Amer.*, vol. 46, no. 1A, p. 105, 1969.

[23] Y. Ohashi, M. Arakawa, J. Kushibiki, B. M. Epelbaum, and A. Winnacker, "Ultrasonic microspectroscopy characterization of AlN single crystals," *Appl. Phys. Express*, vol. 1, no. 7, p. 077004, Jul. 2008.

Ko-hei Sano was born in Hokkaido, Japan, in 1993. He received the B.S. and M.S. degrees in engineering from Waseda University, Tokyo, Japan, in 2016 and 2018, respectively.

He is currently with Asahi Glass Company, Ltd., Tokyo. His main research interests include piezoelectric thin film and device.

Mr. Sano received the 2017 Student Paper Competition Award at the 2017 IEEE International Ultrasonics Symposium.

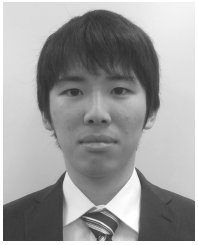

Rei Karasawa was born in Kanagawa, Japan, in 1994. He received the bachelor's degree in engineering from Waseda University, Tokyo, Japan, in 2017, where he is currently pursuing the master's degree.

His main research interests include piezoelectric thin film and crystal growth.

Takahiko Yanagitani was born in Kyoto, Japan, in 1978. He received the Dr.Eng. degree from Doshisha University, Kyoto, in 2006.

He is currently an Associate Professor with Waseda University, Tokyo, Japan. He has authored 11 papers published in the IEEE Transactions on Ultrasonics, Ferroelectrics, and Frequency Control and more than 83 presentations at the IEEE International Ultrasonics Symposium. His main fields of research interests are thin films, piezoelectric devices, and the measurements based on acoustoelectric effects.

Dr. Yanagitani is a member of the IEEE International Ultrasonics Symposium Physical Acoustics Technical Program Committee and the International Workshop on Piezoelectric Materials and Applications in Actuators (IWPMA) Committee. He is currently serving as an Editorial Board Member of *Scientific Reports* (Nature Publishing Group).